PHYSICAL REVIEW C **75**, 054314 (2007)

Pair condensation in a finite Fermi system

M. Sambataro
Istituto Nazionale di Fisica Nucleare-Sezione di Catania, Via S. Sofia 64, I-95123 Catania, Italy
(Received 4 July 2006; published 11 May 2007)

The lowest seniority-zero eigenstates of an exactly solvable multilevel pairing Hamiltonian for a finite Fermi system are examined at different pairing regimes. After briefly reviewing the form of the eigenstates in the Richardson formalism, we discuss a different representation of these states in terms of the collective pairs resulting from the diagonalization of the Hamiltonian in a space of two degenerate time-reversed fermions. We perform a two-fold analysis by working both in the fermionic space of these collective pairs and in a space of corresponding elementary bosons. On the fermionic side, we monitor the variations which occur, with increasing the pairing strength, in the structure of both these collective pairs and the lowest eigenstates. On the bosonic side, after reviewing a fermion-boson mapping procedure, we construct exact images of the fermion eigenstates and study their wave function. The analysis allows a close examination of the phenomenon of pair condensation in a finite Fermi system and gives new insights into the evolution of the lowest (seniority-zero) excited states of a pairing Hamiltonian from the unperturbed regime up to a strongly interacting one.

DOI: 10.1103/PhysRevC.75.054314 PACS number(s): 21.60.−n, 74.20.−z

I. INTRODUCTION

Pairing lies at the heart of quantum many-body physics. In spite of its long history (fundamental works such as those of Mayer [1], Flowers [2], and Racah and Talmi [3] in nuclear physics and that of Bardeen, Cooper, and Schrieffer [4] in condensed matter physics all date back to the 1950s), pairing is still a highly topical subject due to its key role in modeling the structure of a large variety of systems which are the object of current research (see, e.g., Ref. [5] for a recent analysis of pairing in nuclear systems).

Pairing affects both finite and infinite systems. The BCS approximation [4] turns out to be quite appropriate for the latters. In finite systems (such as nuclei and ultrasmall metallic grains, for example), the BCS description of pairing is instead known to lack of reliability as a result of the particle number violation inherent in the BCS wave function. Although more sophisticated approaches, such as the number-projected BCS approximation [6], for example, do exist, none of them has revealed to be as simple and effective as BCS in infinite systems.

In this paper, wishing to investigate the properties of the eigenstates of a pairing Hamiltonian without resorting to approximate methods, we have focused our attention on an exactly solvable pairing model which has received a great deal of attention over the years, namely the so-called reduced BCS [7] or picket-fence [8] model. Applications of this model to finite systems range from nuclear physics, where it has been used as a prototype of a deformed nucleus [9–11], to condensed matter physics, where it has been largely employed to describe the superconducting properties of ultrasmall metallic grains (see Ref. [7] for a comprehensive review article on this subject). Moreover, being quite sensitive to any violation of the Pauli principle, the reduced BCS model has often been used as an ideal testing ground for many-body approximations such as the random phase approximation and its extensions [8,11–15]. Recent analysis of the model can be found in Refs. [16,17].

The exact solutions of the reduced BCS Hamiltonian were discussed in the 1960s in a series of articles by Richardson [9,18–21], also in collaboration with Sherman [22], in the context of nuclear physics. In the Richardson formalism, any seniority-zero eigenstate of this Hamiltonian is a product of collective pair operators characterized by amplitudes which depend on some parameters, the so-called pair energies. These are determined by solving a set of coupled nonlinear equations. Although exact, the Richardson formalism does not offer a straightforward understanding of the structure of the eigenstates. With increasing the pairing strength, as a result of the appearence of singularities in the above equations, some pair energies, two by two, turn into complex-conjugate pairs. No matter what pairing strength, the Richardson eigenstates remain a product of distinct collective pair operators, some of which may then be characterized by complex amplitudes. The purpose of this paper is that of providing a simpler and more intuitive description of the pairing eigenstates and of their evolution at different pairing regimes.

Our analysis will have a two-fold aspect, a fermionic and a bosonic one. From the fermionic point of view, we will define a new set of collective pair operators in terms of which we will reformulate the exact eigenstates. We will therefore study the evolution of these pairs as well as that of the eigenstates. The bosonic analysis will instead be made in terms of elementary bosons, each boson replacing a collective pair. We will review a mapping procedure to transfer the description of the original Fermi system onto the space of these elementary bosons and we will construct an exact image of the fermion eigenstates which will eventually be examined. This work will allow a close examination of the phenomenon of pair condensation in a finite Fermi system and give new insights into the evolution of the lowest (seniority-zero) excited states of a pairing Hamiltonian from the unperturbed regime up to a strongly interacting one.

The paper is organized as follows. In Sec. II, we describe the model and its exact solutions in the Richardson formalism. In Sec. III, we reformulate the eigenstates in terms of a new

set of collective pair operators and study their evolution. In Sec. IV, we carry out the analysis in terms of elementary bosons. All the calculations presented up to this point refer to a system of 12 particles distributed over 12 levels. In Sec. V, we discuss some results referring to other systems. In Sec. VI, we summarize the results and draw some conclusions.

II. THE RICHARDSON FORMALISM

The starting point of our work is the Hamiltonian [7,8]

$$H = \sum_{j=1}^{\Omega} \epsilon_j N_j - g \sum_{i,j=1}^{\Omega} P_i^\dagger P_j, \tag{1}$$

where

$$N_j = \sum_{\sigma} a_{j\sigma}^\dagger a_{j\sigma}, \quad P_j^\dagger = a_{j+}^\dagger a_{j-}^\dagger, \quad P_j = (P_j^\dagger)^\dagger. \tag{2}$$

This Hamiltonian describes a system of fermions distributed over a set of Ω doubly degenerate single particle levels and interacting via a pairing force with a level-independent strength g. We restrict our analysis to the case of an even number of particles ($2N$) and assume equally spaced single-particle energies of the form $\epsilon_j = jd, d$ being the level spacing. The operator $a_{j\sigma}^\dagger$ ($a_{j\sigma}$) creates (annihilates) a fermion in the single-particle state (j, σ), where j identifies one of the Ω levels of the model and $\sigma = \pm$ labels time reversed states. These operators obey standard fermion commutation relations. We exclude partial occupation of the levels, i.e., levels are considered as either fully occupied (two particles in time reversed states) or empty. Singly occupied levels decouple from the rest and are said to be "blocked" [22] since they do not participate in the pair-scattering generated by the Hamiltonian (1). Our model space therefore includes only seniority-zero states [22].

The derivation of the exact eigenstates and eigenvalues of the Hamiltonian (1) is extensively discussed in Refs. [9,18,19,22]. We refer to these publications for a careful study of the subject. Here, we only resume a few basic results of these works. It has been shown by Richardson that a state $|\Psi\rangle$ of the form

$$|\Psi\rangle = \prod_{i=1}^{N} B_i^\dagger |0\rangle, \quad B_i^\dagger = \sum_{k=1}^{\Omega} \frac{1}{2\epsilon_k - E_i} P_k^\dagger \tag{3}$$

is a seniority-zero (unnormalized) eigenstate of the Hamiltonian (1) if the N parameters E_i (the so-called pair energies) are roots of the set of N coupled nonlinear equations

$$1 - \sum_{k=1}^{\Omega} \frac{g}{2\epsilon_k - E_i} + \sum_{l(l\neq i)=1}^{N} \frac{2g}{E_l - E_i} = 0. \tag{4}$$

The eigenvalue $E^{(\Psi)}$ associated with $|\Psi\rangle$ is just the sum of the corresponding pair energies, i.e.,

$$E^{(\Psi)} = \sum_{i=1}^{N} E_i. \tag{5}$$

The numerical solution of Eq. (4) meets some technical difficulties. Indeed, with increasing the strength g of the pairing interaction, it happens that two (real) pair energies E_i become equal thus giving rise to a singularity. When this occurs, these energies turn from real into complex-conjugate pairs. It is in order to handle only real quantities that Richardson introduced some new variables ξ_λ and η_λ [9]. In the case of the ground state, these are defined such that

$$E_{2\lambda-1} = \xi_\lambda - i\eta_\lambda, \quad E_{2\lambda} = \xi_\lambda + i\eta_\lambda \quad (\lambda = 1, 2, \ldots, N/2). \tag{6}$$

This transformation actually holds only for even N but the case of odd N can also be taken into account by assuming that one pair energy is real and the remaining $N-1$ pair energies occur in complex-conjugate pairs [9]. In Eq. (6), ξ_λ is assumed to be always real while η_λ can be either pure imaginary (corresponding to real and distinct $E_{2\lambda-1}$ and $E_{2\lambda}$) or real (corresponding to complex conjugates pair energies). Once the transformation (6) is made, Eqs. (4) depend only on the real quantities ξ_λ and η_λ^2 which can therefore be calculated numerically (although at the cost of a further change of variables [9]).

As an illustrative example, in Fig. 1 we show the ground state pair energies which are obtained in the case $2N = \Omega = 12$. All the calculations which will be discussed up to Sec. IV refer to this system. In Sec. V, we will examine some other systems. The pairing strength is varied in the interval $(0, 2)$ (in units of d). All pair energies turn out to be real up to $g = 0.39$, namely up to the singular point where $E_5 = E_6$. At this point, E_5 and E_6 become complex-conjugate pairs. The same happens to the pair energies E_3 and E_4 at $g = 0.60$ and to E_1 and E_2 at $g = 0.89$. Beyond these singular points only the real part ξ_λ relative to each pair $E_{2\lambda-1}$, $E_{2\lambda}$ is plotted (dash-dotted lines).

The solution of Eqs. (4) in the case of the first excited state requires (besides a different choice of "boundary conditions" [9]) a different definition of the transformation (6) which now

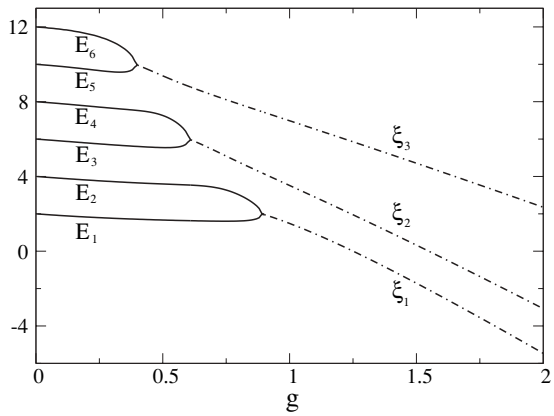

FIG. 1. Pair energies relative to the ground state (solid lines). The energies are real up to the points where $E_{2\lambda-1} = E_{2\lambda}$ ($\lambda = 1, 2, 3$). From there on, they turn into complex-conjugate pairs of the type of Eq. (6) and only their real part ξ_λ is shown (dash-dotted lines). All values are in units of d.

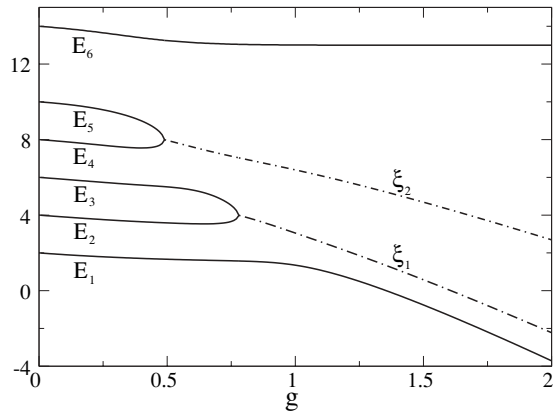

FIG. 2. Pair energies relative to the first excited state (solid lines). Similarly to Fig. 1, dash-dotted lines refer to their real part ξ_λ [see Eq. (7)]. All values are in units of d.

becomes

$$E_{2\lambda} = \xi_\lambda + i\eta_\lambda, \quad E_{2\lambda+1} = \xi_\lambda - i\eta_\lambda, \quad (\lambda = 1, 2, \ldots, N/2-1)$$
$$E_1 = \xi_{N/2} + i\eta_{N/2}, \quad E_N = \xi_{N/2} - i\eta_{N/2}. \tag{7}$$

In Fig. 2, we show the pair energies which are derived in this case. The basic difference with respect to the ground state (Fig. 1) consists in the behavior of the lowest and highest pair energies which are now always real. Therefore, as evident from Figs. 1 and 2, in the Richardson formalism both the ground state and the first excited state are always products of N *distinct* pair operators $B_i^\dagger$, some of which, depending on the pairing strength, may be characterized by complex pair energies.

III. REFORMULATING THE RICHARDSON EIGENSTATES

The complex-conjugate form of the pair energies which enter into the definition of the ground state and the first excited state (but the discussion is actually not limited to these states [9]) guarantees that these states can be easily reformulated in a real form. In the case of the ground state, for example, one has that

$$|\Psi\rangle = \prod_{\lambda=1}^{N/2} B_{2\lambda-1}^\dagger B_{2\lambda}^\dagger |0\rangle \tag{8}$$

(it is hereafter assumed that N is even) and, by making use of the definition (6), one finds

$$B_{2\lambda-1}^\dagger B_{2\lambda}^\dagger = (\Gamma_\lambda^\dagger)^2 + \eta_\lambda^2 (\Theta_\lambda^\dagger)^2, \tag{9}$$

where

$$\Gamma_\lambda^\dagger = \sum_{k=1}^{\Omega} \frac{2\epsilon_k - \xi_\lambda}{(2\epsilon_k - \xi_\lambda)^2 + \eta_\lambda^2} P_k^\dagger, \tag{10}$$

$$\Theta_\lambda^\dagger = \sum_{k=1}^{\Omega} \frac{1}{(2\epsilon_k - \xi_\lambda)^2 + \eta_\lambda^2} P_k^\dagger. \tag{11}$$

The pair operators $\Gamma_\lambda^\dagger$ and $\Theta_\lambda^\dagger$ only depend on the real coefficients ξ_λ and η_λ^2 and the same is true for the product $B_{2\lambda-1}^\dagger B_{2\lambda}^\dagger$ (9). Equation (9) therefore provides a tool to rewrite the Richardson ground state in a real form no matter what g. As a result, this state may be expressed as a linear combination of states which are products of the operators $\Gamma_\lambda^\dagger$ and $\Theta_\lambda^\dagger$. Similar considerations hold also in the case of the transformation (7).

Each eigenstate being characterized by a different set of pairs $(\Gamma_\lambda^\dagger, \Theta_\lambda^\dagger)$, a description of the system in terms of these collective pairs is bound to remain, however, undesirably complicated and unclear. Moreover, no more than Ω linearly independent pairs can actually be constructed in the model space under examination. An unified description of all eigenstates in terms of a single set of (at most) Ω pairs is certainly to be preferred. This is what we have done in this work by choosing as a set of linearly independent pairs those which result from the diagonalization of H in the space $\{P_i^\dagger|0\rangle\}$. We will comment in the following on some consequences of this choice. These pairs, say $\Pi_\rho^\dagger$, are therefore such that

$$\langle 0|\Pi_\rho \Pi_{\rho'}^\dagger|0\rangle = \delta_{\rho\rho'}, \quad \langle 0|\Pi_\rho H \Pi_{\rho'}^\dagger|0\rangle = \tilde{\epsilon}_\rho \delta_{\rho\rho'}. \tag{12}$$

The formulation of each eigenstate $|\Psi\rangle$ in terms of $\Pi_\rho^\dagger$ can be done, in principle, by expressing the pairs $\Gamma_\lambda^\dagger$ and $\Theta_\lambda^\dagger$ in terms of $\Pi_\rho^\dagger$ or, more simply, by diagonalizing H in the space

$$F = \{\Pi_{\rho_1}^\dagger \Pi_{\rho_2}^\dagger \cdots \Pi_{\rho_N}^\dagger |0\rangle \equiv |\rho\rangle\}_{1 \leqslant \rho_1 \leqslant \cdots \leqslant \rho_N \leqslant \Omega}. \tag{13}$$

It is worth noticing that the number of states $|\rho\rangle$ of F is by far larger than the actual dimensionality of the model space under discussion [given by the binomial coefficient $\binom{\Omega}{N}$]. A diagonalization of the overlap matrix in F allows, however, to define a set of $\binom{\Omega}{N}$ basis states which can therefore be used to construct the exact spectrum of the Hamiltonian.

The pairs $\Pi_\rho^\dagger$ are by construction linear combination of the pairs $P_k^\dagger$, i.e., $\Pi_\rho^\dagger = \sum_{k=1}^{\Omega} p(k,\rho) P_k^\dagger$. In Fig. 3, we

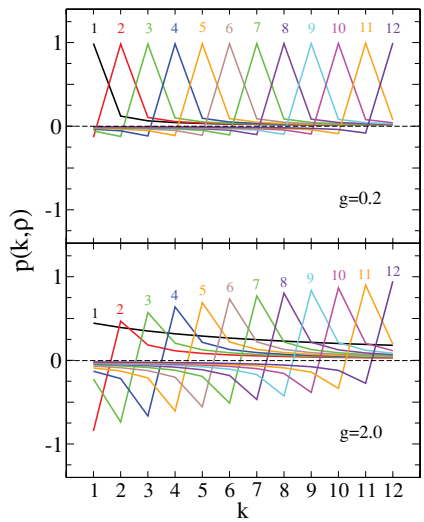

FIG. 3. (Color online) Amplitudes $p(k,\rho)$ characterizing the collective pairs $\Pi_\rho^\dagger$ $(1 \leqslant \rho \leqslant 12)$ for two values of the pairing strength g. The pairs $\Pi_\rho^\dagger$ are ordered for increasing values of their energy $\tilde{\epsilon}_\rho$.

plot the amplitudes $p(k, \rho)$ (they are normalized such that $\sum_k p(k, \rho)^2 = 1$) characterizing each of the $N = 12$ pairs $\Pi^\dagger_\rho$ of the system under study and for two pairing strengths, namely $g = 0.2$ ("weak" coupling) and $g = 2.0$ ("strong" coupling). The pairs $\Pi^\dagger_\rho$ are ordered for increasing values of their energy $\tilde{\epsilon}_\rho$. The behavior of the amplitudes $p(k, \rho)$ appears quite different in the two cases. For $g = 0.2$ (upper panel), all curves exhibit a sharp maximum very close to 1 (in absolute value), thus denoting a very low degree of collectivity of the pairs $\Pi^\dagger_\rho$. These can essentially be identified with the corresponding pairs $P^\dagger_\rho$. For $g = 2.0$ (lower panel), all pairs appear to be more spread out over the single particle levels and, in particular, one pair clearly stands out from all others for its very smooth behavior of $p(k, \rho)$. This is the pair corresponding to the lowest eigenvalue $\tilde{\epsilon}_\rho$ [see Eq. (12)], i.e., the pair $\Pi^\dagger_1$. It is worth noticing that this pair, differently from all others, is also characterized by amplitudes all carrying the same sign.

It is interesting to examine the energies $\tilde{\epsilon}_\rho$ of these pairs. They are shown in Fig. 4 by the solid lines. As a reference, in the same figure, the dashed lines show the unperturbed pair energies, namely the energies of these pairs at $g = 0$. The difference between $\tilde{\epsilon}_\rho$ and the corresponding unperturbed pair energy defines the binding energy of the pair $\Pi^\dagger_\rho$. All pairs appear to be bound at any g but $\Pi^\dagger_1$ exhibits a binding energy which, in the strong coupling region, by far exceeds that of the remaining pairs.

Although we have so far illustrated the features of all possible Ω pairs $\Pi^\dagger_\rho$ that one can construct and introduced a space F built in terms of these, we remark that the exact spectrum of H can also be obtained by working in subspaces of F which involve only a restricted set of pairs $\Pi^\dagger_\rho$. In the case under study ($\Omega = 2N = 12$), for example, it is already sufficient to include pairs $\Pi^\dagger_\rho$ up to $\rho = 9$. In order to simplify the numerical calculations we have constrained our analysis within such a subspace of F (hereafter $\widetilde{F}$).

Moving from the weak to the strong coupling region, significant changes are expected to occur not only in the structure of the pairs $\Pi^\dagger_\rho$ but also in that of the eigenstates $|\Psi\rangle$. Monitoring these changes is, however, not straightforward

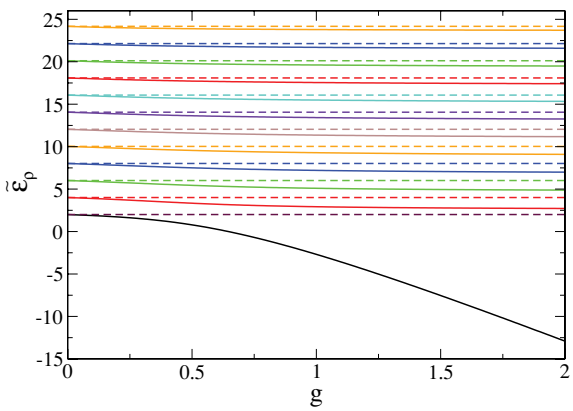

FIG. 4. (Color online) Energies $\tilde{\epsilon}_\rho$ of the pairs $\Pi^\dagger_\rho$ as defined in Eq. (12) (solid lines). The dashed lines show the energies of the same pairs at $g = 0$. All values are in units of d.

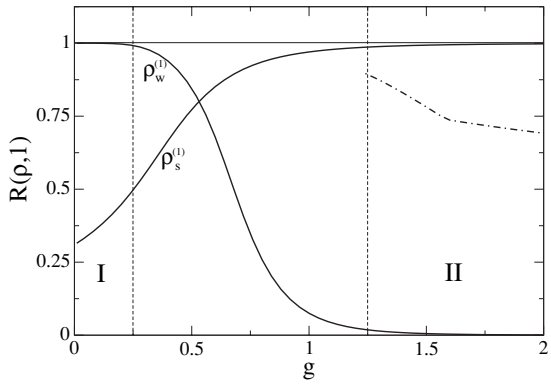

FIG. 5. The quantity $R(\rho, 1)$ discussed in the text for the states $|\rho^{(1)}_w\rangle = \Pi^\dagger_1\Pi^\dagger_2\Pi^\dagger_3\Pi^\dagger_4\Pi^\dagger_5\Pi^\dagger_6|0\rangle$ and $|\rho^{(1)}_s\rangle = (\Pi^\dagger_1)^6|0\rangle$. The dash-dotted line shows the maximum values reached by the remaining $R(\rho, 1)$'s in region II.

due to the composite nature of the operators $\Pi^\dagger_\rho$. In order to follow the evolution of the lowest eigenstates with increasing the pairing strength, we have examined the overlaps between these and all the states $|\rho\rangle$ of $\widetilde{F}$. In particular, we have focused our attention on the lowest four eigenstates $|\Psi_\nu\rangle$ ($\nu = 1, 4$) and we have examined the quantity $R(\rho, \nu) = |\langle\overline{\rho}|\Psi_\nu\rangle|$, $|\overline{\rho}\rangle$ hereafter representing the state $|\rho\rangle$ properly normalized. For each eigenstate $|\Psi_\nu\rangle$, we have searched for the states $|\rho^{(\nu)}_w\rangle$ and $|\rho^{(\nu)}_s\rangle$ corresponding to a maximum of $R(\rho, \nu)$ in the regions of weak and strong coupling, respectively. The evolution of $R(\rho, \nu)$ for $\rho = \rho^{(\nu)}_w$ and $\rho = \rho^{(\nu)}_s$ has therefore been studied.

As far as the ground state is concerned, at small g's, the maximum of $R(\rho, 1)$ is found for $|\rho^{(1)}_w\rangle = \Pi^\dagger_1\Pi^\dagger_2\Pi^\dagger_3\Pi^\dagger_4\Pi^\dagger_5\Pi^\dagger_6|0\rangle$ while, at large g's, for $|\rho^{(1)}_s\rangle = (\Pi^\dagger_1)^6|0\rangle$. The behavior of $R(\rho^{(1)}_w, 1)$ and $R(\rho^{(1)}_s, 1)$ as a function of g is shown in Fig. 5 by the lines labeled $\rho^{(1)}_w$ and $\rho^{(1)}_s$, respectively. For $g \lesssim 0.25$ (hereafter region I), one has $R(\rho^{(1)}_w, 1) \approx 1$. Since $\Pi^\dagger_i \to P^\dagger_i$ when $g \to 0$ (see Fig. 2), in this limit, $|\Psi_1\rangle$ approaches (as expected) the unperturbed ground state of the system, namely the state with the lowest six orbitals fully occupied and the remaining ones empty. For $g \gtrsim 1.25$ (hereafter region II), one has instead $R(\rho^{(1)}_w, 1) \approx 0$, i.e., $|\Psi_1\rangle$ has basically no overlap with $|\rho^{(1)}_w\rangle$. In the same region, $R(\rho^{(1)}_s, 1)$ reaches a value very close to 1 [one finds $R(\rho^{(1)}_s, 1) = 0.998$ at $g = 2.0$] after having rapidly increased from an initial value of 0.31 at $g \approx 0$ [we remark that $R(\rho^{(1)}_s, 1)$ is undefined at $g = 0$ due to the Pauli principle which forbids the existence of $|\rho^{(1)}_s\rangle$]. Because of the nonorthogonality of the states $|\rho\rangle$, the fact that $R(\rho^{(1)}_s, 1) \approx 1$ does not imply that the remaining values $R(\rho, 1)$ can be neglected. As shown in Fig. 5, however, the maximum value of $R(\rho, 1)$ among all remaining states is considerably lower than $R(\rho^{(1)}_s, 1)$ (see the dash-dotted line) and, contrary to the latter, keeps decreasing with increasing g.

We have also evaluated the correlation energy of the state $|\rho^{(1)}_s\rangle$ (namely the difference between the energy of this state and that of the unperturbed ground state) and compared it with the corresponding energy of the ground state. The relative difference is shown in Fig. 6 and it is seen to rapidly approach zero with increasing g. At $g = 2.0$, this difference

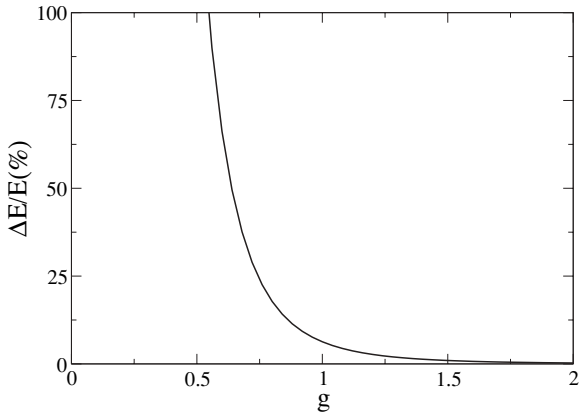

FIG. 6. Relative difference between the correlation energy of the state $|\rho_s^{(1)}\rangle = (\Pi_1^\dagger)^6|0\rangle$ (properly normalized) and the corresponding energy of the ground state (in percent).

is 0.26% whereas the minimum relative difference found in correspondence with the remaining states $|\rho\rangle$ does not get lower than 33.6%. All these results [which, by the way, become more and more pronounced beyond the range (0,2) of the strength g examined so far] support the conclusion that, with increasing g, the ground state is approaching a state of the form $(\Pi_1^\dagger)^6|0\rangle$, namely a condensate of the pair $\Pi_1^\dagger$. This picture of the ground state is noticeably different from that which one has in terms of the Richardson pairs $B_i^\dagger$.

A question which naturally arises at this stage is how $\Pi_1^\dagger$ compares with the pair defining the ground state in the BCS approximation. The BCS ground state is indeed, by construction, a linear combination of condensates of collective pairs, each condensate carrying a different number of pairs. The BCS pair has the form $\Pi_{\rm BCS}^\dagger = \sum_k p_k^{\rm (BCS)} P_k^\dagger$, the amplitudes $p_k^{\rm (BCS)}$ being proportional to the ratio v_k/u_k of the coefficients which define the quasi-particle operator $\alpha_{k\sigma}^\dagger = u_k a_{k\sigma}^\dagger - v_k a_{k-\sigma}$. For the sake of brevity, we avoid discussing the details of the BCS formalism for which we rather address to standard textbooks (see, e.g., Ref. [23]). We also refer to Ref. [24] for an analysis of the BCS approximation within the present model. Here, we only confine ourselves to comparing the amplitudes of the pairs $\Pi_1^\dagger$ and $\Pi_{\rm BCS}^\dagger$. These are shown in Fig. 7 for two values of the pairing strength: $g = 1.5$ (upper panel) and $g = 2.0$ (lower panel). The two pairs exhibit very close amplitudes (their difference decreasing with increasing g) in spite of the fact that the BCS approximation works rather badly in the model under study [24]. The two strengths of Fig. 7 both belong to region II. In region I, on one hand, the BCS approximation does not provide any nontrivial solution (these are found only for $g \gtrsim 0.32$) and, on the other hand, no form of condensation in the ground state emerges in the formalism of the pairs $\Pi_i^\dagger$. No comparison is therefore possible in this region.

As far as the first excited state is concerned, at small g's, the maximum of $R(\rho, 2)$ is found for $|\rho_w^{(2)}\rangle = \Pi_1^\dagger\Pi_2^\dagger\Pi_3^\dagger\Pi_4^\dagger\Pi_5^\dagger\Pi_7^\dagger|0\rangle$ while, at large g's, for $|\rho_s^{(2)}\rangle = (\Pi_1^\dagger)^5\Pi_7^\dagger|0\rangle$. The behavior of $R(\rho_w^{(2)}, 2)$ and $R(\rho_s^{(2)}, 2)$ as a function of g is shown in Fig. 8 by the lines labeled $\rho_w^{(2)}$ and

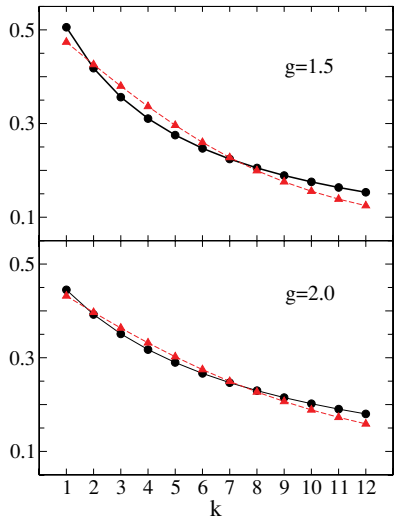

FIG. 7. (Color online) Amplitudes of the pairs $\Pi_1^\dagger$ (circles) and $\Pi_{\rm BCS}^\dagger$ (triangles) for two values of the pairing strength g.

$\rho_s^{(2)}$, respectively. As expected, for $g \to 0$, the first excited state approaches the configuration $P_1^\dagger P_2^\dagger P_3^\dagger P_4^\dagger P_5^\dagger P_7^\dagger|0\rangle$ which corresponds to the lowest seniority-zero excitation in absence of interaction. In region II, instead, the first excited state evolves torward the condensate $(\Pi_1^\dagger)^5\Pi_7^\dagger|0\rangle$. This evolution is, however, definitively less rapid than that observed for the ground state. As in the case of the ground state, in region II, the maximum value of $R(\rho, 2)$ among all remaining states is considerably lower than $R(\rho_s^{(2)}, 2)$ and, contrary to the latter, keeps decreasing with increasing g (dashed-dotted line).

The condensate $|\rho_s^{(2)}\rangle$ differs from $|\rho_s^{(1)}\rangle$ for the presence of the pair $\Pi_7^\dagger$ replacing a pair $\Pi_1^\dagger$. Simple considerations based on the energies $\tilde{\epsilon}_\rho$ of the pairs would have rather suggested as more likely the appearence of the pair $\Pi_2^\dagger$ which is the one immediately above $\Pi_1^\dagger$ (though separated by a large gap) and considerably lower than $\Pi_7^\dagger$ (see Fig. 4). As it can be seen in Fig. 8, instead, the quantity $R(\rho, 2)$ for $|\rho\rangle = (\Pi_1^\dagger)^5\Pi_2^\dagger|0\rangle$

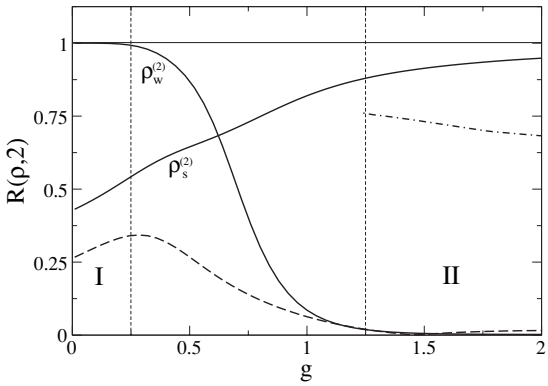

FIG. 8. The quantity $R(\rho, 2)$ discussed in the text for the states $|\rho_w^{(2)}\rangle = \Pi_1^\dagger\Pi_2^\dagger\Pi_3^\dagger\Pi_4^\dagger\Pi_5^\dagger\Pi_7^\dagger|0\rangle$ and $|\rho_s^{(2)}\rangle = (\Pi_1^\dagger)^5\Pi_7^\dagger|0\rangle$. The dash-dotted line shows the maximum values reached by the remaining $R(\rho, 2)$'s in region II. The dashed line refers to $R(\rho, 2)$ for $|\rho\rangle = (\Pi_1^\dagger)^5\Pi_2^\dagger|0\rangle$.

(dashed line) remains very close to zero throughout region II therefore denoting the absence of any appreciable contribution of this component to the structure of the first excited state at large g's. We will further comment in Sec. V on such an interesting outcome.

The analysis of the second and third excited states turns out to be more involved than those carried out so far. The reason is that these states happen to be exactly degenerate and this degeneracy does not allow an unambigous definition of their wave functions. Indeed, if $|\Psi_3\rangle$ and $|\Psi_4\rangle$ are the eigenstates (with energies $E^{(\Psi_3)} = E^{(\Psi_4)} \equiv E^{(\Psi_{34})}$) which result from a diagonalization of H in $\widetilde{F}$, any other pair of states of the type

$$|\Psi_{34}^{(+)}\rangle = d_3|\Psi_3\rangle + d_4|\Psi_4\rangle,$$
$$|\Psi_{34}^{(-)}\rangle = d_4|\Psi_3\rangle - d_3|\Psi_4\rangle \tag{14}$$

with $d_3^2 + d_4^2 = 1$ (for simplicity we are assuming to handle only real quantities) also represents a pair of eigenstates with the same energy. $|\Psi_{34}^{(+)}\rangle$ and $|\Psi_{34}^{(-)}\rangle$ depend on the coefficients d_3 and d_4 and so does any overlap between them and a generic state $|i\rangle$. Therefore, in this case, an analysis of the structure of the states of the type already discussed for the ground and first excited states needs some additional remarks.

A quantity which does not suffer of any ambiguity related to the degeneracy of $|\Psi_3\rangle$ and $|\Psi_4\rangle$ is

$$\mathcal{M}_i^{(34)} = \langle i|\Psi_3\rangle^2 + \langle i|\Psi_4\rangle^2. \tag{15}$$

$\mathcal{M}_i^{(34)}$ is indeed invariant for the transformation (14). This quantity represents the maximum value that the squared overlap between the generic state $|i\rangle$ and $|\Psi_{34}^{(+)}\rangle$ can reach. This maximum is found in correspondence with the state

$$|\Psi_{i,34}^{(+)}\rangle = \frac{1}{\sqrt{\mathcal{M}_i^{(34)}}}(\langle i|\Psi_3\rangle|\Psi_3\rangle + \langle i|\Psi_4\rangle|\Psi_4\rangle). \tag{16}$$

The paired eigenstate is

$$|\Psi_{i,34}^{(-)}\rangle = \frac{1}{\sqrt{\mathcal{M}_i^{(34)}}}(\langle i|\Psi_4\rangle|\Psi_3\rangle - \langle i|\Psi_3\rangle|\Psi_4\rangle). \tag{17}$$

The latter state is, by construction, such that $\langle i|\Psi_{i,34}^{(-)}\rangle = 0$.

We have monitored the evolution, as a function of the pairing strength, of all the overlaps $\langle\overline{\rho}|\Psi_{\rho,34}^{(+)}\rangle$ for $|\rho\rangle$ belonging to $\widetilde{F}$ and observed, in region II, a maximum in correspondence with the state $|\rho\rangle = (\Pi_1^\dagger)^5\Pi_8^\dagger|0\rangle \equiv |\rho_s^{(+)}\rangle$. We have therefore selected among all possible states of the type (14) the states $|\Psi_{\rho,34}^{(+)}\rangle$ and $|\Psi_{\rho,34}^{(-)}\rangle$ for $\rho = \rho_s^{(+)}$ (hereafter simply $|\Psi^{(+)}\rangle$ and $|\Psi^{(-)}\rangle$). The properties of these states are illustrated in the following.

In Fig. 9, we show the quantity $R(\rho,+) = |\langle\overline{\rho}|\Psi^{(+)}\rangle|$ for two different states: $|\rho\rangle = |\rho_s^{(+)}\rangle$ and $|\rho\rangle = \Pi_1^\dagger\Pi_2^\dagger\Pi_3^\dagger\Pi_4^\dagger\Pi_5^\dagger\Pi_8^\dagger|0\rangle \equiv |\rho_w^{(+)}\rangle$. The behavior of these overlaps closely reminds those of Figs. 5 and 8. The state $|\Psi^{(+)}\rangle$ is seen to approach the configuration $P_1^\dagger P_2^\dagger P_3^\dagger P_4^\dagger P_5^\dagger P_8^\dagger|0\rangle$ for $g \to 0$ (but it should be noticed that, at $g = 0$, $|\Psi^{(+)}\rangle$ is undefined due to the Pauli principle which prevents the state $|\rho_s^{(+)}\rangle$ from existing) and to evolve toward the condensate $(\Pi_1^\dagger)^5\Pi_8^\dagger|0\rangle$ at large g's. In the same figure, the dash-dotted line shows the maximum value among all remaining overlaps.

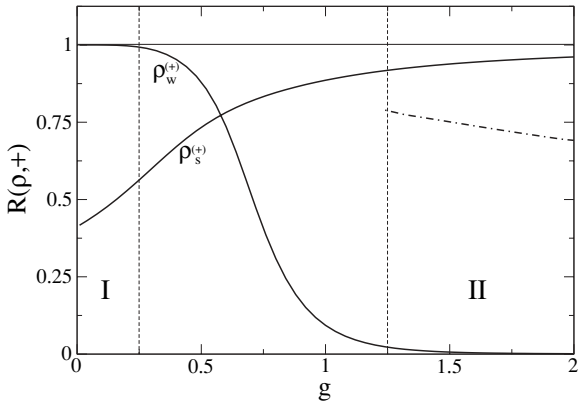

FIG. 9. The quantity $R(\rho,+)$ discussed in the text for the states $|\rho_w^{(+)}\rangle = \Pi_1^\dagger\Pi_2^\dagger\Pi_3^\dagger\Pi_4^\dagger\Pi_5^\dagger\Pi_8^\dagger|0\rangle$ and $|\rho_s^{(-)}\rangle = (\Pi_1^\dagger)^5\Pi_8^\dagger|0\rangle$. The dash-dotted line shows the maximum values reached by the remaining $R(\rho,+)$'s in region II.

As far as the paired eigenstate $|\Psi^{(-)}\rangle$ is concerned, in Fig. 10, we show the quantity $R(\rho,-) = |\langle\overline{\rho}|\Psi^{(-)}\rangle|$ for $|\rho\rangle = (\Pi_1^\dagger)^5\Pi_6^\dagger|0\rangle \equiv |\rho_s^{(-)}\rangle$ and $|\rho\rangle = \Pi_1^\dagger\Pi_2^\dagger\Pi_3^\dagger\Pi_4^\dagger\Pi_6^\dagger\Pi_7^\dagger|0\rangle \equiv |\rho_w^{(-)}\rangle$. The state $|\Psi^{(-)}\rangle$ therefore approaches $P_1^\dagger P_2^\dagger P_3^\dagger P_4^\dagger P_6^\dagger P_7^\dagger|0\rangle$ for $g \to 0$ (but, similarly to $|\Psi^{(+)}\rangle$, it is undefined at $g = 0$ due to the Pauli principle) and evolves torward the condensate $(\Pi_1^\dagger)^5\Pi_6^\dagger|0\rangle$ at large g's. Still in Fig. 10, the dash-dotted line shows the maximum value among all remaining overlaps. Interestingly enough, one finds that $R(\rho_s^{(-)},-)$ is very close (the relative difference being of the order 10^{-5}) to the maximum value that the overlap between the state $|\rho_s^{(-)}\rangle$ and a state of the type (14) can reach. Therefore if, on one side, the state $|\Psi^{(+)}\rangle$ maximizes by construction the overlap with the state $|\rho_s^{(+)}\rangle = (\Pi_1^\dagger)^5\Pi_8^\dagger|0\rangle$, on the other side, one finds that the paired eigenstate $|\Psi^{(-)}\rangle$ maximizes (almost exactly) the overlap with the state $|\rho_s^{(-)}\rangle = (\Pi_1^\dagger)^5\Pi_6^\dagger|0\rangle$. Similarly to what observed in the case of the first excited state, the evolution of $|\Psi^{(+)}\rangle$ and $|\Psi^{(-)}\rangle$ toward the

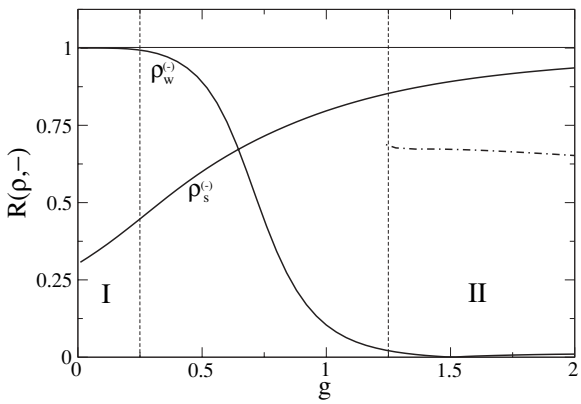

FIG. 10. The quantity $R(\rho,-)$ discussed in the text for the states $|\rho_w^{(-)}\rangle = \Pi_1^\dagger\Pi_2^\dagger\Pi_3^\dagger\Pi_4^\dagger\Pi_6^\dagger\Pi_7^\dagger|0\rangle$ and $|\rho_s^{(-)}\rangle = (\Pi_1^\dagger)^5\Pi_6^\dagger|0\rangle$. The dash-dotted line shows the maximum values reached by the remaining $R(\rho,-)$'s in region II.

respective condensates $(\Pi_1^\dagger)^5\Pi_8^\dagger|0\rangle$ and $(\Pi_1^\dagger)^5\Pi_6^\dagger|0\rangle$ is clear but not as rapid as for the ground state.

It is worthy comparing these results with those which are obtained if one adopts slightly perturbed single-particle energies of the type, for example, $\epsilon_i = (i + i^2/\Omega^3)d$. These single-particle energies are characterized by a spacing not any longer constant but varying from $1.002d$ up to a maximum of $1.013d$. This tiny variation in the spacing is, however, sufficient to remove the degeneracy of $|\Psi_3\rangle$ and $|\Psi_4\rangle$ (at $g = 1$, for example, one finds $E^{(\Psi_3)} = 34.179$ and $E^{(\Psi_4)} = 34.182$ to be compared with the value $E^{(\Psi_{34})} = 33.991$ for the degenerate case). The analysis of this nondegenerate case fully confirms all the results obtained so far. In particular, the overlaps of the eigenstates $|\Psi_3\rangle$ and $|\Psi_4\rangle$ with the states $|\rho_w^{(+)}\rangle$, $|\rho_s^{(+)}\rangle$ and $|\rho_w^{(-)}\rangle$, $|\rho_s^{(-)}\rangle$ turn out to be undistinguishable from those shown in Figs. 9 and 10 for the states $|\Psi^{(+)}\rangle$ and $|\Psi^{(-)}\rangle$.

IV. THE BOSONIC APPROACH

The description of the lowest eigenstates of the Hamiltonian (1) given so far, both in the Richardson formalism and in the formulation of Sec. III, has required handling objects (the collective pairs) which have a composite nature. This inevitably makes the analysis of the wave functions rather difficult. In this section, we discuss a different approach which is instead based on the use of "elementary" objects, namely of bosons characterized by commutation relations of the type $[b_i, b_{i'}^\dagger] = \delta_{ii'}$, $[b_i, b_{i'}] = 0$. Each elementary boson replaces a collective pair. This formalism has the merit of allowing a more transparent analysis of the states. In Sec. IV A, we review the mapping procedure that we use to transfer the description of the system from the original space of the collective pairs onto the space of the elementary bosons. In Sec. IV B, we discuss the results which are obtained in the new formalism.

A. The mapping procedure

The problem of mapping a system of composite objects (such as the pairs $\Pi_i^\dagger$) onto a space of corresponding elementary objects (such as the bosons $b_i^\dagger$) is a well known one and can be tackled in several ways (see, e.g., Ref. [25] for a review on the subject). The approach that we have adopted in this work retains the basic principles of that discussed in Ref. [26] and closely follows its revised form recently discussed in Ref. [15]. With respect to the latter, the present formulation refers to a more general case. Being based on a correspondence between fermion and boson states and on the equality between corresponding matrix elements, the approach follows the philosophy of the Marumori method [27,28].

We try to keep the formalism as general as possible. Let therefore $\mathcal{P}_i^\dagger$ be a generic collective pair creation operator. The index i is supposed to run from 1 up to a maximum value $N^{(1)}$. We define the space

$$\begin{aligned}\mathcal{F}^{(n)} &= \{\mathcal{P}_{k_1}^\dagger \mathcal{P}_{k_2}^\dagger \cdots \mathcal{P}_{k_n}^\dagger|0\rangle\}_{1\leqslant k_1\leqslant k_2\leqslant\cdots\leqslant k_n\leqslant N^{(1)}} \\ &\equiv \{|n,k\rangle\}_{1\leqslant k\leqslant N^{(n)}}. \end{aligned} \tag{18}$$

This can be seen as a generalization of the space F of Eq. (13). The set of $N^{(n)}$ states $|n,k\rangle$ is, in general, nonorthonormal. In order to single out a subset of orthonormal states, we diagonalize the overlap matrix $\langle n,i|n,j\rangle$. Let $\mathcal{N}_j^{(n)}$ and $f_{ij}^{(n)}$ be the eigenvalues and eigenfunctions, respectively, which results from this diagonalization. They are such that

$$\sum_l \langle n,i|n,l\rangle f_{lj}^{(n)} = \mathcal{N}_j^{(n)} f_{ij}^{(n)}, \tag{19}$$

$$\sum_i f_{ij}^{(n)} f_{ij'}^{(n)} = \delta_{jj'}, \quad \sum_j f_{ij}^{(n)} f_{i'j}^{(n)} = \delta_{ii'}. \tag{20}$$

In general, only $\widetilde{N}^{(n)}$ eigenvalues ($\widetilde{N}^{(n)} < N^{(n)}$) turn out to be different from zero and, correspondingly, we introduce the states

$$|\widetilde{n,k}\rangle = \begin{cases} \frac{1}{\sqrt{\mathcal{N}_k^{(n)}}}\sum_i f_{ik}^{(n)}|n,i\rangle, & 1\leqslant k\leqslant \widetilde{N}^{(n)} \\ \sum_i f_{ik}^{(n)}|n,i\rangle, & \widetilde{N}^{(n)}+1\leqslant k\leqslant N^{(n)} \end{cases}. \tag{21}$$

According to such a definition, the first $\widetilde{N}^{(n)}$ states $|\widetilde{n,k}\rangle$ are orthonormal while the remaining ones are zero norm states.

In correspondence with any operator $\mathcal{P}_i^\dagger$, we introduce an elementary boson operator $b_i^\dagger$ of the type discussed above. Let also $|0\rangle$ be the boson vacuum. Similarly to the fermion space $\mathcal{F}^{(n)}$, we introduce the boson space

$$\begin{aligned}\mathcal{B}^{(n)} &= \left\{\frac{1}{\sqrt{M_\rho}} b_{k_1}^\dagger b_{k_2}^\dagger \cdots b_{k_n}^\dagger|0\rangle\right\}_{1\leqslant k_1\leqslant k_2\leqslant\cdots\leqslant k_n\leqslant N^{(1)}} \\ &\equiv \{|n,k\rangle\}_{1\leqslant k\leqslant N^{(n)}}, \end{aligned} \tag{22}$$

where M_ρ is a normalization factor. A one-to-one correspondence exists between the states of $\mathcal{F}^{(n)}$ and $\mathcal{B}^{(n)}$, the basic difference being, however, that the states $|n,k\rangle$ are already orthonormal. In correspondence with the states $|\widetilde{n,k}\rangle$, we introduce the new set of boson states (still orthonormal)

$$|\widetilde{n,k}\rangle = \sum_i f_{ik}^{(n)}|n,i\rangle, \quad 1\leqslant k\leqslant N^{(n)} \tag{23}$$

and define the transformation operator

$$\begin{aligned} V &= |0\rangle\langle 0| + \sum_{k_1=1}^{N^{(1)}} |\widetilde{1,k_1}\rangle\langle\widetilde{1,k_1}| + \sum_{k_2=1}^{N^{(2)}} |\widetilde{2,k_2}\rangle\langle\widetilde{2,k_2}| + \cdots \\ &\equiv \sum_n \sum_{k_n=1}^{N^{(n)}} |\widetilde{n,k_n}\rangle\langle\widetilde{n,k_n}|. \end{aligned} \tag{24}$$

The boson image of a fermion operator T is defined as

$$T_B = VTV^\dagger = \sum_{n,k_n}\sum_{n',k_{n'}} |\widetilde{n,k_n}\rangle\langle\widetilde{n,k_n}|T|\widetilde{n',k_{n'}}\rangle\langle\widetilde{n',k_{n'}}|. \tag{25}$$

As a first remark, we observe that T_B is hermitian if so is T. If, in particular, the fermion operator conserves the particle number, as in the case of a generic Hamiltonian $\mathcal{H}$, Eq. (25) gives

$$H_B = \sum_n \sum_{k,k'} |\widetilde{n,k}\rangle\langle\widetilde{n,k}|\mathcal{H}|\widetilde{n,k'}\rangle\langle\widetilde{n,k'}|. \tag{26}$$

Let us point out some properties of H_B. It follows from Eq. (26) that

$$(\widetilde{n,k}|H_B|\widetilde{n,k'}) = \langle \widetilde{n,k}|\mathcal{H}|\widetilde{n,k'}\rangle. \tag{27}$$

This equality implies that, for each n, the diagonalization of H_B in the full space of states $|n,k)$ [or, equivalently, $|\widetilde{n,k})$] will result in $\widetilde{N}^{(n)}$ "physical" eigenvalues identical to the fermion ones plus $N^{(n)} - \widetilde{N}^{(n)}$ "spurious" eigenvalues which are exactly zero. As it is evident from Eq. (27), the presence of these extra eigenvalues is related to the existence of $N^{(n)} - \widetilde{N}^{(n)}$ zero norm states $|\widetilde{n,k}\rangle$. Furthermore, one sees that no mixing is possible between physical and spurious eigenstates.

By making use of Eqs. (19) and (20), one also derives from the equality (27)

$$(n,l|H_B|n,m) = \sum_{ij} R^{(n)}_{li}\langle n,i|\mathcal{H}|n,j\rangle R^{(n)}_{jm}, \tag{28}$$

with

$$R^{(n)}_{li} = \sum_{k=1}^{\widetilde{N}^{(n)}} f^{(n)}_{lk}\frac{1}{\sqrt{\mathcal{N}^{(n)}_k}} f^{(n)}_{ik}. \tag{29}$$

Equation (28) directly relates the matrix elements of H_B in $\mathcal{B}^{(n)}$ with those of H in $\mathcal{F}^{(n)}$. An expression of the form of Eq. (28) can also be found in Ref. [29].

The definition (25) of the image T_B involves the boson states $|\widetilde{n,k})$. In order to find an explicit expression of T_B in terms of boson operators only, one needs to express the projection operator $|0)(0|$ as a function of $b^\dagger, b$. This can be done by first noticing that

$$1 = |0)(0| + \sum_{k_1} b^\dagger_{k_1}|0)(0|b_{k_1} + \sum_{k_1\leqslant k_2}\frac{1}{1+\delta_{k_1k_2}} b^\dagger_{k_1}b^\dagger_{k_2}|0)(0|b_{k_1}b_{k_2} + \cdots \tag{30}$$

and therefore proceeding iteratively. At the first step, it is

$$|0)(0| = 1 - \sum_{k_1} b^\dagger_{k_1}|0)(0|b_{k_1} - \sum_{k_1\leqslant k_2}\frac{1}{1+\delta_{k_1k_2}} b^\dagger_{k_1}b^\dagger_{k_2}|0)(0|b_{k_1}b_{k_2} - \cdots \tag{31}$$

and by substituting this in Eq. (30) one derives

$$|0)(0| = 1 - \sum_k b^\dagger_k b_k + O(4), \tag{32}$$

where, in general, by $O(n)$, we mean terms with at least n operators $b^\dagger, b$ arranged in normal order with respect to the boson vacuum $|0)$. The iteration proceeds by inserting Eq. (32) again in Eq. (31) and so on up to the desired level of complexity of $|0)(0|$.

B. Numerical results

Let us apply the mapping procedure just described to the system under study. We assume $\mathcal{P}^\dagger_i = \Pi^\dagger_i$ and, consistently with what done so far, we restrict the set of these pairs to the lowest 9. In such a case, the space $\mathcal{F}^{(6)}$ of Eq. (18) simply reduces to the space $\widetilde{F}$ defined in Sec. III. In order to fulfill the equality (27) [or Eq. (28)] up to $n = 6$, the boson Hamiltonian H_B has to carry, in general, up to six-body terms. Due to the fact that the pairs $\Pi^\dagger_i$ diagonalize the Hamiltonian [see Eq. (12)], the simplest of these terms, i.e., the one-body term, turns out to be diagonal. The choice of formulating the eigenstates in terms of these pairs rather than directly in terms of the pairs $\Gamma^\dagger_\lambda, \Theta^\dagger_\lambda$ has been made also in such a perspective. In this case, the energies $\tilde{\epsilon}_i$ acquire the meaning of single-boson energies and the boson Hamiltonian takes the form $H_B = \sum_i \tilde{\epsilon}_i b^\dagger_i b_i + V_B$, V_B being an interaction term which contains, in general, up to six-body operators. A Hamiltonian of this type qualitatively reminds that of well known phenomenological models such as the interacting boson model (IBM) [30].

On the basis of the properties of the mapping procedure illustrated in the previous subsection, the diagonalization of H_B in $\mathcal{B}^{(6)}$ is expected to result in a physical spectrum identical to that of H in $\widetilde{F}$ plus some spurious eigenvalues. The explicit construction of the physical eigenstates can be carried out in a straightforward way by taking advantage of the calculations already performed in the fermion space $\widetilde{F}$. By keeping the same notation used in the previous subsection, a generic fermion eigenstate $|\Psi_\nu\rangle$ can be written as

$$|\Psi_\nu\rangle = \sum_{k=1}^{\widetilde{N}^{(6)}} \tilde{c}^{(\nu)}_k|\widetilde{6,k}\rangle = \sum_{i=1}^{N^{(6)}}\left(\sum_{k=1}^{\widetilde{N}^{(6)}}\frac{1}{\sqrt{\mathcal{N}^{(6)}_k}} f^{(6)}_{ik}\tilde{c}^{(\nu)}_k\right)|6,i\rangle. \tag{33}$$

Due to the equality of Eq. (27), the corresponding boson eigenstate is simply

$$|\Psi_\nu) = \sum_{k=1}^{\widetilde{N}^{(6)}} \tilde{c}^{(\nu)}_k|\widetilde{6,k}) = \sum_{i=1}^{N^{(6)}}\left(\sum_{k=1}^{\widetilde{N}^{(6)}} f^{(6)}_{ik}\tilde{c}^{(\nu)}_k\right)|6,i) \equiv \sum_i c^{(\nu)}_i|6,i). \tag{34}$$

From the knowledge of the coefficients $f^{(6)}_{ik}$ and $\tilde{c}^{(\nu)}_k$, it is therefore immediate to construct the amplitudes $c^{(\nu)}_i$ which define the boson image $|\Psi_\nu)$.

The analysis of the eigenstates in terms of elementary bosons is undoubtedly simpler than that in terms of collective pairs. As in the fermionic case, the analysis has concerned the lowest four eigenstates. For each $|\Psi_\nu)$, we have searched for the largest (in absolute values) amplitudes $c^{(\nu)}_i$ in the regions of weak and strong coupling. We denote these amplitudes $c^{(\nu)}_w$ and $c^{(\nu)}_s$, respectively. As far as the ground state is concerned, in Fig. 11 we show the amplitudes $|c^{(1)}_w|$ and $|c^{(1)}_s|$. These turn out to be associated with the components $b^\dagger_1b^\dagger_2b^\dagger_3b^\dagger_4b^\dagger_5b^\dagger_6|0)$ and $\frac{1}{\sqrt{6!}}(b^\dagger_1)^6|0)$, respectively. These components are the bosonic counterparts of the states $|\rho^{(1)}_w\rangle$ and $|\rho^{(1)}_s\rangle$ introduced in Sec. III and the behavior of $|c^{(1)}_w|$ and $|c^{(1)}_s|$ indeed reminds that of the corresponding fermionic quantities $R(\rho^{(1)}_w, 1)$ and $R(\rho^{(1)}_s, 1)$ shown in Fig. 5. At very small values of g one finds $|c^{(1)}_w| \simeq 1$

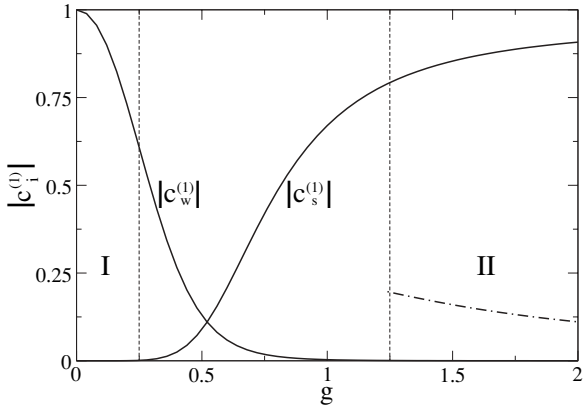

FIG. 11. Absolute values of the amplitudes $c_w^{(1)}$ and $c_s^{(1)}$ associated with the components $b_1^\dagger b_2^\dagger b_3^\dagger b_4^\dagger b_5^\dagger b_6^\dagger|0\rangle$ and $\frac{1}{\sqrt{6!}}(b_1^\dagger)^6|0\rangle$, respectively, of the boson ground state $|\Psi_1\rangle$. The dashed-dotted line shows the maximum value reached by the remaining amplitudes $|c_i^{(1)}|$ in region II.

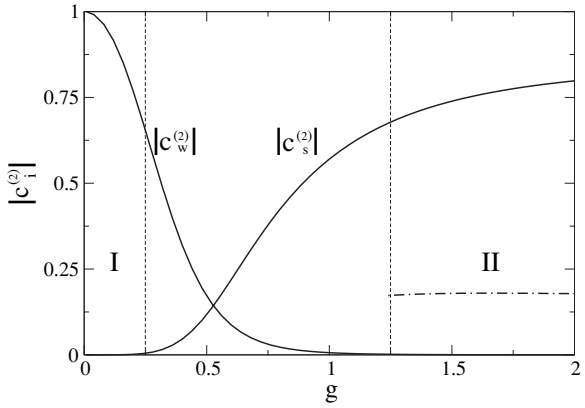

FIG. 12. Absolute values of the amplitudes $c_w^{(2)}$ and $c_s^{(2)}$ associated with the components $b_1^\dagger b_2^\dagger b_3^\dagger b_4^\dagger b_5^\dagger b_7^\dagger|0\rangle$ and $\frac{1}{\sqrt{5!}}(b_1^\dagger)^5 b_7^\dagger|0\rangle$, respectively, of the boson first excited state $|\Psi_2\rangle$. The dashed-dotted line shows the maximum values reached by the remaining amplitudes $|c_i^{(2)}|$ in region II.

and, due to the normalization condition $\sum_i c_i^2 = 1$, this implies that $|\Psi_1\rangle \simeq b_1^\dagger b_2^\dagger b_3^\dagger b_4^\dagger b_5^\dagger b_6^\dagger|0\rangle$. Therefore, in spite of their nature which would allow them to share the same level, the bosons $b_i^\dagger$ each occupy a different level. This reflects the fact that, in this region, the bosons $b_i^\dagger$ are associated with pairs $\Pi_i^\dagger$ with a very low degree of collectivity (see Fig. 2, upper panel). Consequently, the underlying fermionic structure plays a crucial role and the Pauli principle, whose presence in the boson space is guaranteed by the many-body structure of the boson Hamiltonian, severely affects the behavior of these bosons. The amplitude $|c_w^{(1)}|$ rapidly goes to zero with increasing g and, correspondingly, $c_s^{(1)}$ rises up by reaching values larger than 0.9 at $g \approx 2$. In region II, the boson ground state thus becomes largely dominated by the condensate $(b_1^\dagger)^6|0\rangle$, the boson $b_1^\dagger$ corresponding to the highly collective, deeply bound pair $\Pi_1^\dagger$. The Pauli principle no longer manifests itself explicitly in this region. Still in Fig. 11, the dashed-dotted line shows the maximum values reached by the remaining amplitudes $|c_i^{(1)}|$ in region II.

The behavior of $|c_w^{(\nu)}|$ and $|c_s^{(\nu)}|$ for the three lowest excited states is shown in Figs. 12–14. Figure 12 refers to the first excited state. The amplitudes $c_w^{(2)}$ and $c_s^{(2)}$ plotted in this figure are found in correspondence with the components $b_1^\dagger b_2^\dagger b_3^\dagger b_4^\dagger b_5^\dagger b_7^\dagger|0\rangle$ and $\frac{1}{\sqrt{5!}}(b_1^\dagger)^5 b_7^\dagger|0\rangle$, respectively, of $|\Psi_2\rangle$. As far as the second and third excited states are concerned, the analysis has been carried out according to the same criteria discussed for the corresponding fermion eigenstates. This has lead to the definition of a pair of eigenstates $|\Psi^{(+)}\rangle$ and $|\Psi^{(-)}\rangle$, exactly analogous to $|\Psi^{(+)}\rangle$ and $|\Psi^{(-)}\rangle$, whose basic features are illustrated in Figs. 13 and 14. The amplitudes $c_w^{(+)}$ and $c_s^{(+)}$ turn out to be associated with the components $b_1^\dagger b_2^\dagger b_3^\dagger b_4^\dagger b_5^\dagger b_8^\dagger|0\rangle$ and $\frac{1}{\sqrt{5!}}(b_1^\dagger)^5 b_8^\dagger|0\rangle$, respectively. The amplitudes $c_w^{(-)}$ and $c_s^{(-)}$ are instead found in correspondence with the components $b_1^\dagger b_2^\dagger b_3^\dagger b_4^\dagger b_6^\dagger b_7^\dagger|0\rangle$ and $\frac{1}{\sqrt{5!}}(b_1^\dagger)^5 b_6^\dagger|0\rangle$, respectively. In Figs. 12–14, the dashed-dotted line shows the maximum values reached by the remaining amplitudes $|c_i^{(\nu)}|$ in region II.

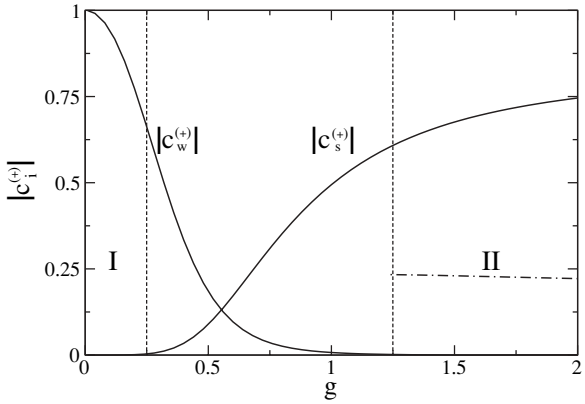

FIG. 13. Absolute values of the amplitudes $c_w^{(+)}$ and $c_s^{(+)}$ associated with the components $b_1^\dagger b_2^\dagger b_3^\dagger b_4^\dagger b_5^\dagger b_8^\dagger|0\rangle$ and $\frac{1}{\sqrt{5!}}(b_1^\dagger)^5 b_8^\dagger|0\rangle$, respectively, of the boson state $|\Psi^{(+)}\rangle$ (see text). The dashed-dotted line shows the maximum values reached by the remaining amplitudes $|c_i^{(+)}|$ in region II.

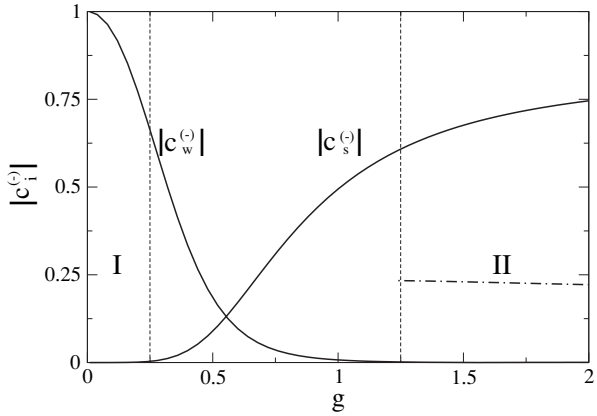

FIG. 14. Absolute values of the amplitudes $c_w^{(-)}$ and $c_s^{(-)}$ associated with the components $b_1^\dagger b_2^\dagger b_3^\dagger b_4^\dagger b_6^\dagger b_7^\dagger|0\rangle$ and $\frac{1}{\sqrt{5!}}(b_1^\dagger)^5 b_6^\dagger|0\rangle$, respectively, of the boson state $|\Psi^{(-)}\rangle$ (see text). The dashed-dotted line shows the maximum values reached by the remaining amplitudes $|c_i^{(-)}|$ in region II.

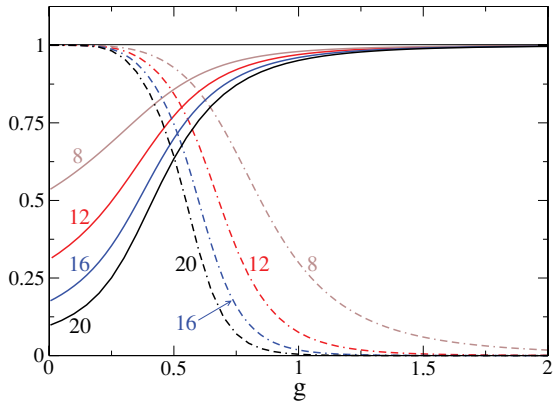

FIG. 15. (Color online) Overlaps between the ground state and the condensate $(\Pi_1^\dagger)^N|0\rangle$ (solid line) and between the ground state and the state $\Pi_1^\dagger\Pi_2^\dagger\cdots\Pi_N^\dagger|0\rangle$ (dashed-dotted line) for systems with different number of particles (shown next to each line).

The behaviours of the amplitudes of the bosonic eigenstates which are illustrated in the above figures are fully consistent with the results of the fermionic analysis of Sec. III. One observes an evolution of the three lowest excited states toward states which are largely dominated by condensates of the type $(b_1^\dagger)^5 b_\alpha^\dagger|0\rangle$. In particular, one finds $\alpha = 7$ for the first excited state and $\alpha = 8$ and $\alpha = 6$ for the (degenerate) second and third excited states $|\Psi^{(+)}\rangle$ and $|\Psi^{(-)}\rangle$. As it is clearly visible in these figures and as it has also been observed in the fermionic analysis, the above evolution is, however, definitely less rapid than that observed in the case of the ground state.

V. OTHER SYSTEMS

All the calculations discussed so far have referred to a system of $2N = 12$ particles distributed over $\Omega = 12$ levels. Performing the same kind of calculations for larger systems becomes soon difficult due to the rapidly growing size of the matrices involved. However, taking advantage of the knowledge of the Richardson ground state obtained by solving Eqs. (4), it has been possible to perform some calculations also for systems with $2N = 16$ and $2N = 20$ particles (still distributed over $\Omega = 2N$ levels). In particular, we have evaluated the overlap between the ground state and the condensate $(\Pi_1^\dagger)^N|0\rangle$ as well as the overlap between the ground state and the state $\Pi_1^\dagger\Pi_2^\dagger\cdots\Pi_N^\dagger|0\rangle$. The corresponding results are shown in Fig. 15. For completeness, we have included in the same figure the results for the system with $2N = 12$ already shown in Fig. 5 and we have also added those referring to the smaller system with $2N = 8$. The behaviours of these overlaps are all similar but, as a major result, one may notice that the evolution toward the condensed phase becomes sharper and sharper with increasing the number of particles.

VI. SUMMARY AND CONCLUSIONS

This paper has been devoted to an analysis of the lowest seniority-zero eigenstates of the reduced BCS Hamiltonian for a finite Fermi system. We have first briefly reviewed the form of these eigenstates in the Richardson formalism: they are a product of distinct collective pair operators, some of which, depending on the pairing strength, may be characterized by complex amplitudes. We have therefore attempted an alternative and (in our purposes) more transparent description of these states in terms of a new set of collective pairs. These are the pairs resulting from the diagonalization of the Hamiltonian in a space of two degenerate time-reversed fermions. We have first discussed the evolution, as a function of the pairing strength, of both these pairs and the lowest eigenstates for a system of 12 particles distributed over 12 levels.

With increasing g, we have observed the formation of a pair markedly different from all others for its high degree of collectivity and its large binding energy: this is the lowest pair $\Pi_1^\dagger$. This pair has been found very similar to that resulting in the BCS approximation. The numerical analysis has clearly pointed out the existence of two well distinct regimes, one at small g's (the region I) characterized by eigenstates which are basically a product of distinct, poorly collective, weakly bound pairs and one at large g's (the region II) characterized instead by different condensates of $\Pi_1^\dagger$. As far as the ground state is concerned, we have observed an evolution toward the condensate $(\Pi_1^\dagger)^6|0\rangle$ while for the three lowest excited states condensates of the type $(\Pi_1^\dagger)^5\Pi_\lambda^\dagger|0\rangle$ with $\lambda = 6, 7, 8$ have emerged. The evolution toward the condensed phase has turned out to be faster in the case of the ground state.

The appearance of the pairs $\Pi_6^\dagger$, $\Pi_7^\dagger$, and $\Pi_8^\dagger$ in the condensates that describe the main components of the three lowest excited states may seem somewhat surprising since other pairs exist (e.g., $\Pi_2^\dagger$ or $\Pi_3^\dagger$) which have a considerably lower energy. Besides the energy, a crucial difference between the pairs $\Pi_6^\dagger$, $\Pi_7^\dagger$, and $\Pi_8^\dagger$ and lower pairs such as $\Pi_2^\dagger$ or $\Pi_3^\dagger$ can be found in the distribution of their amplitudes: this is peaked at or above the Fermi level for $\Pi_6^\dagger$, $\Pi_7^\dagger$, and $\Pi_8^\dagger$ and at the lowest single particle levels for $\Pi_2^\dagger$ or $\Pi_3^\dagger$. This different distribution has manifestly favored the pairs $\Pi_6^\dagger$, $\Pi_7^\dagger$, and $\Pi_8^\dagger$ by allowing them to overcome the handicap represented by their higher energy.

In the recent past, truncated nuclear shell model calculations have been performed by working in spaces spanned by some sets of collective pairs (see, e.g., [31] and references therein). These pairs have been constructed by diagonalizing the Hamiltonian in spaces of two nucleons outside the closed shells and by selecting (for given spin and isospin) the pairs solely on the basis of their energy. The results of the present work clearly show, however, that energy is not the only parameter that should be considered for a correct selection of the pairs and that a more comprehensive criterium taking also into account the structure of the pairs should rather be devised.

We have also performed a complementary analysis of the lowest eigenstates of the reduced BCS Hamiltonian by working in a purely bosonic framework, each boson being the image of a collective pair. After reviewing a mapping procedure, we have constructed an exact image of the lowest eigenstates which have therefore been examined. This approach has lead to conclusions in full agreement with those of the fermionic

analysis by offering, as an advantage, a more direct access to the structure of the states.

In the bosonic approach, increasing the pairing strength has resulted in a marked variation of the single boson energies (equal by construction to the energies of the above collective pairs) which have passed from an equally spaced distribution (at small g's) up to a distribution characterized by a large gap between the lowest level and the remaining ones (at large g's). Correspondingly, the occupancy of the boson levels has passed from an uniform one (one boson per level) up to a pronounced boson condensation on the lowest level. The two regimes already observed in the fermionic analysis have thus clearly manifested themselves in the bosonic case as well. Although not very sharply defined, the regions of the pairing strength at which these different regimes occur are consistent with those resulting from the analysis of Ref. [17]. Calculations performed (but only at the fermionic level and for the ground state) for systems up to $2N = 20$ particles distributed over $\Omega = 20$ levels have all provided results similar to the corresponding ones for $2N = \Omega = 12$ by evidencing an evolution toward the condensed phase which becomes sharper and sharper with increasing the number of particles.

ACKNOWLEDGMENTS

The author wishes to thank G. Angilella, D. Gambacurta, and P. Schuck for very useful discussions on this subject.

[1] M. G. Mayer, Phys. Rev. **78**, 16 (1950); **78**, 22 (1950).
[2] B. H. Flowers, Proc. R. Soc. London A **212**, 248 (1952).
[3] G. Racah and I. Talmi, Physica **18**, 1097 (1952).
[4] J. Bardeen, L. N. Cooper, and J. R. Schrieffer, Phys. Rev. **108**, 1175 (1957).
[5] D. J. Dean, Rev. Mod. Phys. **75**, 607 (2003).
[6] P. Ring and P. Schuck, *The Nuclear Many-Body Problem* (Springer-Verlag, Berlin, 1980).
[7] J. von Delft and D. C. Ralph, Phys. Rep. **345**, 61 (2001).
[8] J. G. Hirsch, A. Mariano, J. Dukelsky, and P. Schuck, Ann. Phys. (NY) **296**, 187 (2002).
[9] R. W. Richardson, Phys. Rev. **141**, 949 (1966).
[10] M. Guttormsen, A. Bjerve, M. Hjorth-Jensen, E. Melby, J. Rekstad, A. Schiller, S. Siem, and A. Belić, Phys. Rev. C **62**, 024306 (2000).
[11] J. Dukelsky, G. G. Dussel, J. G. Hirsch, and P. Schuck, Nucl. Phys. **A714**, 63 (2003).
[12] J. Dukelsky and P. Schuck, Phys. Lett. **B464**, 164 (1999).
[13] A. Storozhenho, P. Schuck, J. Dukelsky, G. Röpke, and A. Vdovin, Ann. Phys. (NY) **307**, 308 (2003).
[14] N. Dinh Dang, Phys. Rev. C **71**, 024302 (2005).
[15] D. Gambacurta, M. Sambataro, and F. Catara, Phys. Rev. C **73**, 014310 (2006).
[16] E. A. Yuzbashyan, A. A. Baytin, and B. L. Altshuler, Phys. Rev. B **68**, 214509 (2003).
[17] M. B. Barbaro, R. Cenni, S. Chiacchiera, A. Molinari, and F. Palumbo, arXiv:nucl-th/0602070.
[18] R. W. Richardson, Phys. Lett. **3**, 277 (1963).
[19] R. W. Richardson, J. Math. Phys. **6**, 1034 (1965).
[20] R. W. Richardson, Phys. Rev. **144**, 874 (1966).
[21] R. W. Richardson, Phys. Rev. **159**, 792 (1967).
[22] R. W. Richardson and N. Sherman, Nucl. Phys. **52**, 221 (1964).
[23] D. J. Rowe, *Nuclear Collective Motion* (Methuen and Co. Ltd, London, 1970).
[24] R. W. Richardson, Phys. Lett. **14**, 325 (1965).
[25] A. Klein and E. R. Marshalek, Rev. Mod. Phys. **63**, 375 (1991).
[26] M. Sambataro, Phys. Rev. C **52**, 3378 (1995).
[27] T. Marumori, M. Yamamura, and A. Tokunaga, Prog. Theor. Phys. **31**, 1009 (1964).
[28] T. Marumori, M. Yamamura, A. Tokunaga, and K. Takada, Prog. Theor. Phys. **32**, 726 (1964).
[29] C. W. Johnson and J. N. Ginocchio, Phys. Rev. C **50**, R571 (1994).
[30] F. Iachello and A. Arima, *The Interacting Boson Model* (Cambridge University Press, Cambridge, 1987).
[31] E. Kwaśniewicz, F. Catara, and M. Sambataro, J. Phys. G: Nucl. Part. Phys. **23**, 911 (1997).